Self-presentation

I. **Name and surname**

Dawid Piątkowski

II. **Diplomas obtained, academic/artistic degrees – including the titles, place and year of issue, and the title of doctoral thesis.**

- November 2008

  Ph.D. in Physics,
  Faculty of Physics, Astronomy and Informatics,
  Nicolaus Copernicus University in Toruń

  Title of thesis: *„ Measurement and interpretation of two-step absorption processes in rare earths doped materials"* – with distinction

- April 2004

  M.Sc. in Physics,
  Faculty of Physics, Astronomy and Informatics,
  Nicolaus Copernicus University in Toruń

  Title of thesis: *„Spectral properties of prototype optical fibers activated by neodymium. Microspherical lasers"*

III. **Information concerning employment in scientific/artistic institutions.**

- 2013 – now   assistant Professor   Institute of Physics Nicolaus Copernicus University in Toruń

- 2012-2013   postdoctoral fellow   Department of Chemistry / Center for NanoScience (CeNS) Ludwig Maximilian University of Munich

- 2009-2012   adjunct researcher   Institute of Physics Nicolaus Copernicus University in Toruń

- 2008-2009   assistant researcher   Institute of Physics Nicolaus Copernicus University in Toruń

IV. **Indication of achievements* pursuant to article 16 item 2 of the act of law dated 14 March 2003, concerning scientific titles, and degrees and titles in the domain of art (Official Journal, 2016, item 882 with later amendments)**

a) Title of the scientific/artistic achievement

In accordance with the above, I indicate scientific achievement, which consists of monothematic series of 5 publications, focused on a microscopic view on light up-conversion (from low to high energy) and energy transport processes that occur in α-NaYF$_4$:Er^{3+}/Yb^{3+} nanocrystals interacting with metallic nanoparticles, entitled:

„Conversion and transport of energy in plasmonic hybrid nanostructures"

b) (Author/Authors, title/titles of the publications, including publication date, name of the publisher, reviewers)

[B.P1] N. Mauser, D. Piątkowski, T. Mancabelli, M. Nyk, S. Maćkowski, A. Hartschuh,
„Tip enhancement of upconversion photoluminescence from rare earth ion doped nanocrystals",
ACS Nano, 2015, Volume: 9, Issue: 4, Pages: 3617-3626, IF:13.334

[B.P2] D. Piątkowski, M.K. Schmidt, M. Twardowska, M. Nyk, J. Aizpurua, S. Maćkowski,
„Spectral selectivity of plasmonic interactions between Individual up-converting nanocrystals and spherical gold nanoparticles", Materials, 2017, Volume: 10, Pages: 905-915, IF: 2.654

[B.P3] D. Piątkowski, N. Hartmann, T. Mancabelli, M. Nyk, S. Maćkowski, A. Hartschuh,
„Silver nanowires as receiving-radiating nanoantennas in plasmon-enhanced up-conversion processes", Nanoscale, 2015, Volume: 7, Issue: 4, Pages: 1479-1484, IF:7.760

[B.P4] N. Hartmann, D. Piątkowski, R. Ciesielski, S. Maćkowski, A. Hartschuh,
„Radiation channels close to a plasmonic nanowire visualized by back focal plane imaging",
ACS Nano, 2013, Volume: 7, Issue: 11, Pages: 10257-10262, IF:12.033

[B.P5] A. Prymaczek, M. Cwierzona, J. Grzelak, D. Kowalska, M. Nyk, S. Mackowski, D. Piatkowski,
„Remote activation and detection of up-converted luminescence via surface plasmon polaritons propagating in a silver nanowire",
Nanoscale, 2018, Volume: 10, Issue: 26, Pages: 12841-12847, IF:7.233

c) Description of scientific/artistic objectives of the above work/works and accomplished results, including description of their potential use.

IV.c.1. <u>Introduction</u>

Optical microscopy and spectroscopy of single nanoparticles, such like: molecules, quantum dots, nanocrystals, etc., attract great interest of many research groups around the world. Despite the fact that optical detection of a single molecule has been performed over 30 years ago, luminescence microscopy is still intensively developed [1]. Recently, experimental achievements regarding highly-resolved imaging techniques have been awarded the Nobel Prize in Chemistry in 2014. Indeed, observation of optical response of single nanoemitters gives unique research possibilities. First of all, it eliminates heterogeneity that usually accompanies macroscopic measurements. Observation of single, individual elements, separated from the ensemble, allows to analyze undisturbed physical processes that take place within isolated systems. Therefore, it allows to understand the mechanisms of excitation or quenching of the luminescence, as well as energy transfer or energy dissipation within the smallest physical objects.

Experimental analysis of single nanoobjects would not have been possible without technological development, which has been observed in the last years. High sensitivity of optical detectors, as well as resolution of spectroscopic analyzers, together with excellent precision of mechanical elements, all of these allow construction of better optimized analytical equipment and manipulation of the matter at the nanoscale. Nowadays, it is possible to design, prepare, and investigate completely new class of objects, not observed previously in nature, called hybrid nanostructures. Since they consist of least two, well known but different nanoobjects, the hybrid nanostructure features new physical properties, as well as functionality, which has been never seen before.

Nowadays, especially interesting are plasmonic hybrid nanostructures. Typically, they consist of at least two optically active nanoobjects, one of which is a metallic nanoparticle, and the second is any single emitter like: dye molecule [2], fluorescent protein [3], quantum dot [4], nanocrystal [5], polymer [6], etc. Hybrid nanostructures can be produced using variety of fabrication techniques. The elements can be deposited layer by layer [7], chemically conjugated [8] or mechanically positioned using AFM *(Atomic Force Microscopy)*, optical tweezers [9], etc.

Plasmonic hybrid nanostructures are constructed in order to obtain a new system, featuring modified (improved) or completely new optical properties. To the most interesting and frequently observed changes, that apply to the a single emitter within a hybrid nanostructure, one can include: increase of absorption efficiency, modification of emission rates, spectral broadening of absorption lines, sensitizing to polarized light, and control of photostability of the system. Especially important are the first two effects, whose occurrence (separable or combined) can lead to the luminescence (fluorescence) enhancement phenomenon, called MEF *(Metal Enhanced Fluorescence)* [10].

Observation of the MEF phenomenon is not a trivial task and requires precise optimization of all the elements of the hybrid system. Particularly important is appropriate matching of the metallic nanoparticles to the spectral characteristic of the emitter. Nowadays, the chemical protocols of synthesis, allow to prepare various metallic nanoparticles with different optical properties. Especially popular are nanoparticles made of silver or gold, in shape of nanospheres, nanorods, nanostars, nanowires, etc. Regarding size, shape, and material properties, metallic

nanoparticles can feature different optical properties [11]. Measured absorption spectra, attributed to free electrons oscillations in metal, can feature different spectral shapes and widths. Moreover, maximum of the extinction can be positioned in a different part of the spectrum, from ultraviolet to near-infrared. Exemplary nanoparticles of different shapes, together with corresponding SEM (*Scanning Electron Microscope*) images and extinction spectra are presented in Fig. 1.
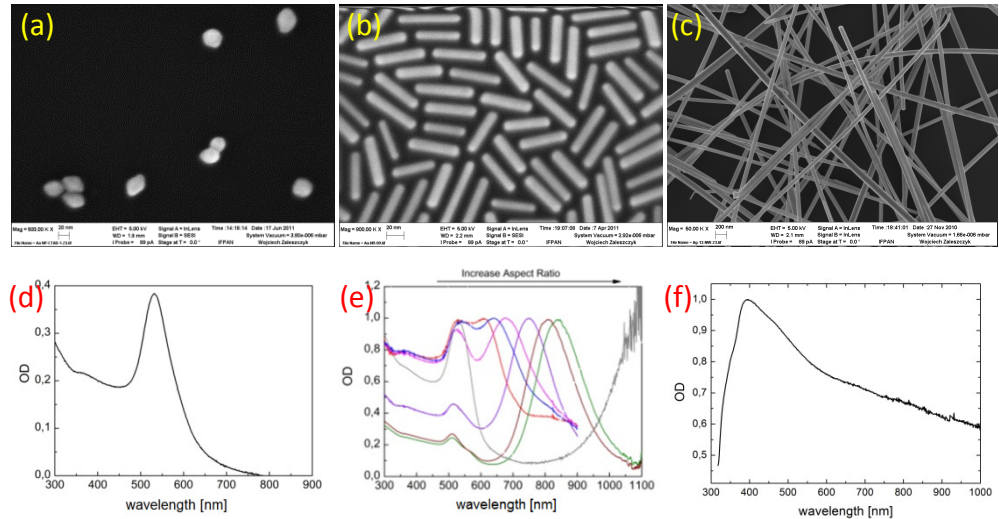

Fig. 1. Exemplary SEM images of the metallic nanoparticles: (a) gold nanospheres, (b) gold nanorods, (c) silver nanowires. Corresponding extinction spectra are presented in sections (d), (e) and (f), respectively. Optical tuning of the extinction spectra of gold nanorods by changing width-to-length aspect ratio, is presented in section (e) [12].

Depending on the size and shape of the metallic nanoparticles, there are two types of electron oscillations that can be activated by light. For small nanoparticles, whose size is much smaller than the wavelength of light, LSPRs (*Localized Surface Plasmon Resonances*) are typically observed. However, in a situation when at last one dimension of the nanoparticle is much larger that the wavelength of light, SPPs (*Surface Plasmon Polaritons*) propagating along metal-dielectric interface can be activated. Interestingly, SPPs can participate in energy dissipation processes and energy transport for distances ranging from a few to even tens of micrometers [13].

Metallic nanoparticles operating within a hybrid nanostructure play a double role. On one hand, properly optimized nanoparticles can very effectively absorb light and localize the excitation energy in the near field ($d_{NF} << \lambda_{exc}$). At the same time, the emitter is exposed to extremely high intensity of the electric field, what – for a spectrally well matched system – can increase excitation efficiency. Consequently, enhanced absorption can lead to an increase of the luminescence intensity, which can be observed until the system is saturated [14]. In the literature, the above process is often called the antenna effect [15].

The second effect contributing to the MEF process is growth of spontaneous emission rates, observed for emitters localized close to a metallic nanoparticle. According to the Fermi's golden rule, probability of the emission depends on the product of squared matrix element and DOS (*Density of States*), which express the ability of the structure surrounding the emitter to support the emitted photons [16]. Metallic nanoparticle placed close to the emitter allows modification of DOS, what – under specific circumstances – can increase radiative emission rates, and as a consequence, effective intensity of the emitted light. This phenomenon has been observed for the first time by E. Purcell at radio frequencies [17]. Nowadays, metallic nanoparticles are widely used for modifying DOS and emission rates of nearby emitters, what is called Radiative Decay Engineering [18].

Several parameters have to be optimized in order to observe MEF phenomenon in a plasmonic hybrid nanostructure. Especially important is optimal spectral matching between elements of the system. To improve absorption of the system, plasmonic resonance should overlap with maxima of absorption of the emitter. This quite intuitive condition guaranties effective absorption of the excitation energy by the hybrid nanostructure. However, metal-induced enhancement of the spontaneous emission rates requires different spectral optimization. According to the systematic experimental research, the largest enhancement of the radiative emission rates is usually observed for a system, where spectral position of the emission line is red-shifted with respect to the maximum of the extinction of metallic nanoparticles [19]. Is such a situation, by introducing large enough spectral offset, the nonradiative energy transfer from the emitter to the metallic nanoparticle – which can quench the luminescence – can be minimized. Another, extremely critical parameter is the distance between the emitter and the metallic nanoparticle. In the experiment, single metallic nanoparticle has precisely approached to the emitter using near field microscope (Fig. 2). It was demonstrated that maximal MEF can be observed for distances between 10 to 15 nm [20]. When the distance is too large, the metal-emitter interaction decreases and the enhancement disappears. On the other hand, when the distance is too small, the luminescence is strongly quenched by nonradiative energy transfer from the emitter to the metallic nanoparticle.
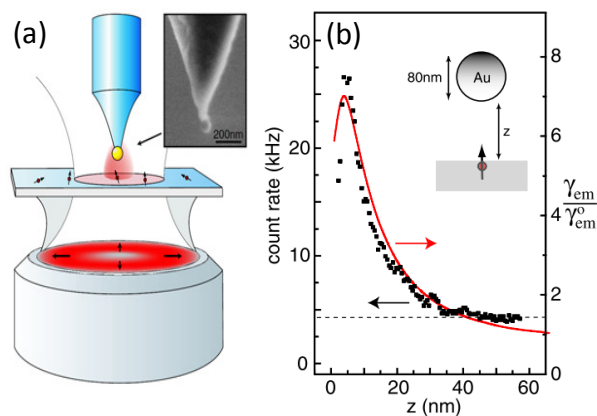

Fig. 2. (a) Demonstration of an experiment where single metallic nanoparticles is precisely approached to a dye molecule. (b) On the graph, the luminescence intensity (rate enhancement) is plotted versus distance between the molecule and metallic nanoparticle [20].

Typically, the increase of a quantum efficiency is the main reason, which justifies the effort for designing and developing plasmonic nanostructures. It recent years, both organic and inorganic emitters (within a hybrid nanostructures) have been considered and analyzed. Of particular interest are REs (*Rare Earths*) doped nanomaterials. In contrast to most of organic and inorganic emitters, REs doped materials feature relatively narrow absorption and emission lines. They can be assigned to intraconfigurational *f↔f* transitions, which have mostly dipole-electric or dipole-magnetic character [21]. One of the most interesting and popular ions are neodymium (Nd^{3+}) and erbium (Er^{3+}). They have been applied in many optoelectronic devices, like advanced laser systems and quantum amplifiers for telecommunication networks [22]. However, true variety of the physical effects – that lead to the radiative emission – are activated by anti-Stokes excitation scheme [23]. In such a situation, energy of the emitted photons is much higher than energy of the excitation ones. The whole process fulfils the energy conservation, since emission of one highly-energetic photon is preceded by sequential absorption of two (or more) low-energetic (infrared) photons, what is illustrated in Fig. 3. The process of visible light emission under infrared excitation is called UC (*Up-conversion*). The largest variety of UC processes have been observed for materials doped with Pr^{3+}, Tm^{3+}, Ho^{3+} and Er^{3+} ions [23].
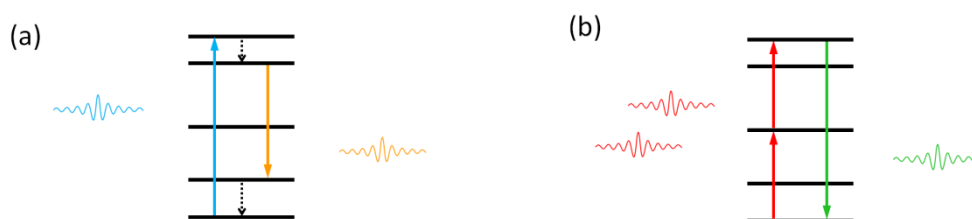

Fig. 3. (a) Illustration of the photoluminescence process observed for Stokes system. Highly-energetic photon is absorbed what leads to the emission of a photon of lower energy. (b) In the anti-Stokes system, emission of light is followed by sequential absorption of low-energetic photons of energies lower that energy of the emitted one.

The up-conversion processes have found numerous applications is science and technology. On one hand, the anti-Stokes excitation can be an alternative mechanism for optical pumping of lasers and telecommunication amplifiers [24]. Some UC processes can find applications in sensors [25]. In the last years, however, of particular interest are various nanomaterials doped with rare earths ions. One of the most interesting and useful applications is UC contrast for biological and medical imaging [26]. Since anti-Stokes luminescence is rarely seen in natural (biological) luminescence systems, the acquired tomograms are free of autofluorescence of tissues and feature high signal to noise ratio (high contrast). Moreover, the infrared excitation, that is exploited in UC luminescence, allows for better tissue penetration depth, what is crucial for medical applications [27]. Quite recently, it has been shown that REs doped nanomaterials can sensitize conductive polymers for infrared radiation [6]. This phenomenon can be used for designing new photovoltaic systems, operating in the infrared.

From the point of view of basic research, rare earths doped nanomaterials are interesting candidates for components of plasmonic hybrid nanostructures. Due to complex excitation mechanisms that lead to anti-Stokes luminescence, as well as variety of potential applications, metal enhanced up-conversion processes are very interesting and important. Influence of a metallic nanoparticle on UC luminescence is much more complex than it is observed for typical (Stokes) luminescence systems. In general, metallic nanoparticle can improve efficiency of multi-photon absorption. Additionally, it can modify spontaneous emission rates of REs ions, which are rather low [28]. At the same time, plasmonic effects cannot disturb interionic energy transfer processes that are fundamental for many up-conversion mechanisms [23]. Until 2010, that is when I got interested in plasmon enhanced up-conversion processes, only basics properties of plasmonic hybrid up-conversion nanostructures have been presented [5][29]. Published results concerned typically highly concentrated samples. Metal enhanced up-conversion processes occurring within single nanostructures have not been examined at this time. The only exception is the experiment wherein position of a single nanocrystal (with respect to a metallic nanoparticle) was controlled by AFM. Authors demonstrated increased intensity of the emission, illustrated by basic spectroscopic analysis [9].

IV.c.2. **Motivation and objectives**

My fascination in up-conversion processes within plasmonic hybrid nanostructures started in 2009, when I joined new research group established by Professor Sebastian Maćkowski in the Institute of Physics, Nicolaus Copernicus University in Torun. Focusing on new research topic I was encouraged to acquire new knowledge regarding optical microscopy of nanostructures. Within two years I have learned basics of the fluorescence microscopy, spectroscopy of single molecules, and plasmonic. Nevertheless, I was aware that advanced research on up-conversion processes that occur in hybrid nanostructures requires unique experimental equipment. Due to financial support of the Ministry of Science and Higher Education under the project *Mobility Plus*, I have completed one year long postdoctoral fellowship in the Department of Chemistry and CeNS (Institute of Physical Chemistry), Ludwig Maximilian University of Munich, under supervision of Professor Achim Hartschuh. During this time, I have learned several new experimental techniques, including high-resolution anit-Stokes near field optical microscopy and Fourier plane optical microscopy. Using these new experimental capabilities, I collected high quality data, giving new insights into up-conversion processes occurring in plasmonic hybrid nanostructures. These results have been published in international journals and are the essence of my scientific achievement. My research were financed by four projects granted by the Ministry of Science and Higher Education (N N202 238940, 633/MOB/2011/0), and the National Science Centre (2013/09/D/ST3/03746, 2017/26/E/ST3/00209).

Research on up-conversion processes within plasmonic nanostructures required well known, efficient and stable nanoemitters. From available materials I chose α-NaYF$_4$ nanocrystals doped with Er^{3+} and Yb^{3+} (2/20 mol%) ions, embedded homogeneously in the volume of nanocrystals. α-NaYF$_4$:Er^{3+}/Yb^{3+} nanocrystals are one of the most stable anti-Stokes emitters. The up-conversion mechanism is well known and is very efficient [23]. Therefore, they can be perceived as exemplary emitters, what makes possible to get insight into details of plasmonic effects. I have received the nanocrystals as a part of long cooperation with Professor Marcin Nyk from Wroclaw University of Technology. The nanocrystals have been prepared using wet chemistry techniques. The average diameter of the nanocrystals was about 20 nm and they were dispersed in chloroform [26]. Exemplary TEM image of α-NaYF$_4$ nanocrystals is presented in Fig. 4a.

In α-NaYF$_4$:Er^{3+}/Yb^{3+} nanocrystals we observe one of the most efficient and well understood mechanism of up-conversion, called ETU (*Energy Transfer Up-conversion*) [23]. In this system, Yb^{3+} ions play the role of donors, transferring excitation energy to Er^{3+}. The most efficient anti-Stokes luminescence guarantees laser excitation at 980 nm, activating $^2F_{7/2} \rightarrow {}^2F_{5/2}$ absorption transition in Yb^{3+}. Subsequently, the energy is nonradiativelly transferred to Er^{3+} in the sequence of following transitions: $^4I_{15/2} \rightarrow {}^4I_{11/2} + {}^4I_{11/2} \rightarrow {}^4F_{7/2}$ and $^4I_{15/2} \rightarrow {}^4I_{11/2} + {}^4I_{13/2} \rightarrow {}^4F_{9/2}$, presented in Fig. 4b. Eventually, Er^{3+} ions are excited to states $^2H_{11/2} + {}^4S_{3/2}$ and $^4F_{9/2}$ and spontaneously emit radiation detected at 540 nm (green) and 650 nm (red), respectively. The excitation mechanism has a multistage character and requires absorption of two quanta of energy. Besides ETU mechanism, nanocrystals can be excited via ESA (*Excited State Absorption*) mechanism, in which two infrared photons are sequentially absorbed directly by Er^{3+} ions [30].
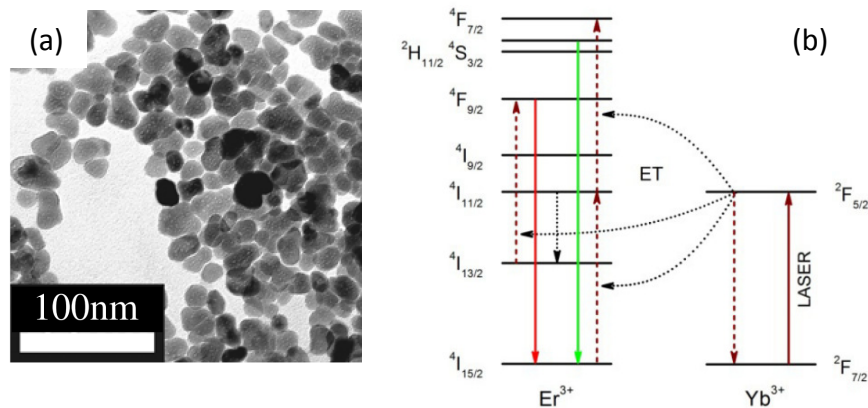

Fig. 4. (a) TEM image of α-NaYF$_4$ nanocrystals. (b) Simplified energy diagram of Er^{3+}/Yb^{3+} system. Brown arrows indicate processes that lead to the anti-Stokes luminescence (green and red arrows) [31].

Functionality of the anti-Stokes emitters is very useful for basic spectroscopic research. In contrast to typical (Stokes) photoluminescence centers, the absorption band is localized in the infrared part of the spectrum, even hundreds of nanometers far from the emission lines. For this reason, the influence of the metallic nanoparticles on absorption and spontaneous emission rates processes can be investigated separately. Moreover, for particular case of Er^{3+}, the excited states $^2H_{11/2}+^4S_{3/2}$ and $^4F_{9/2}$ are populated independently, via separate absorption channels from down to up, what is illustrated in Fig. 4b. As a consequence, metal induced modifications of radiative emission rates from $^2H_{11/2}+^4S_{3/2}$ does not influence significantly population of $^4F_{9/2}$ level, which is excited via independent channel. Therefore, anti-Stokes nanocrystals coupled with properly prepared metallic nanoparticles can give unique opportunity to manipulate radiative emission rates of chosen, interesting transitions. The objective of my work was to analyze up-conversion processes occurring within single plasmonic hybrid nanostructures using advanced techniques of optical microscopy and spectroscopy.

IV.c.3. <u>Methodology</u>

The research equipment, that allows for optical characterization of the plasmonic hybrid nanostructures, is confocal fluorescence (luminescence) microscope. The microscope was a core component of three experimental setups, which were used during my research. Two microscopes (LMU and NCU) have been designed and assembled by myself. The third setup (LMU), dedicated for near field experiments, was upgraded by myself and adapted to specific spectral requirements of the anti-Stokes materials. All experimental setups mentioned above, shared the same basics functionality, which is photoluminescence imaging of single nanostructures together with spectral and time-resolved characterization of the emission. The microscope built in the Institute of Physics NCU is still operating and being upgraded in order to meet new experimental challenges. Photography of the experimental setup, together with exemplary results, is presented in Fig. 5.

Schematics of the experimental setup is presented in Fig. 5b. The samples are prepared by depositing (i.e. spin coating) nanoparticles on top of a glass coverslip. Then, it is mounted on a sample holder, coupled with a piezo-electric table (Physikalische Instrumente, P-561). The sample can be raster-scanned with spatial resolution of about 1 nm. High numerical aperture oil objective is used (Nikon, CFI Apo TIRF NA=1.49) and is mounted under the sample (inverted microscope). For the excitation source is a single-mode continuous wave semiconductor laser operating at 980 nm (Spectra-Laser) and the optical power is about 10 mW is used. The laser beam focused by the objective on the surface of the sample form a small spot of diameter about 400 nm. Size of the spot determines spatial resolution of the imaging [32]. Light emitted by the nanocrystal is collected by the objective and propagates to avalanche photodiode, mounted in the single photon counting unit
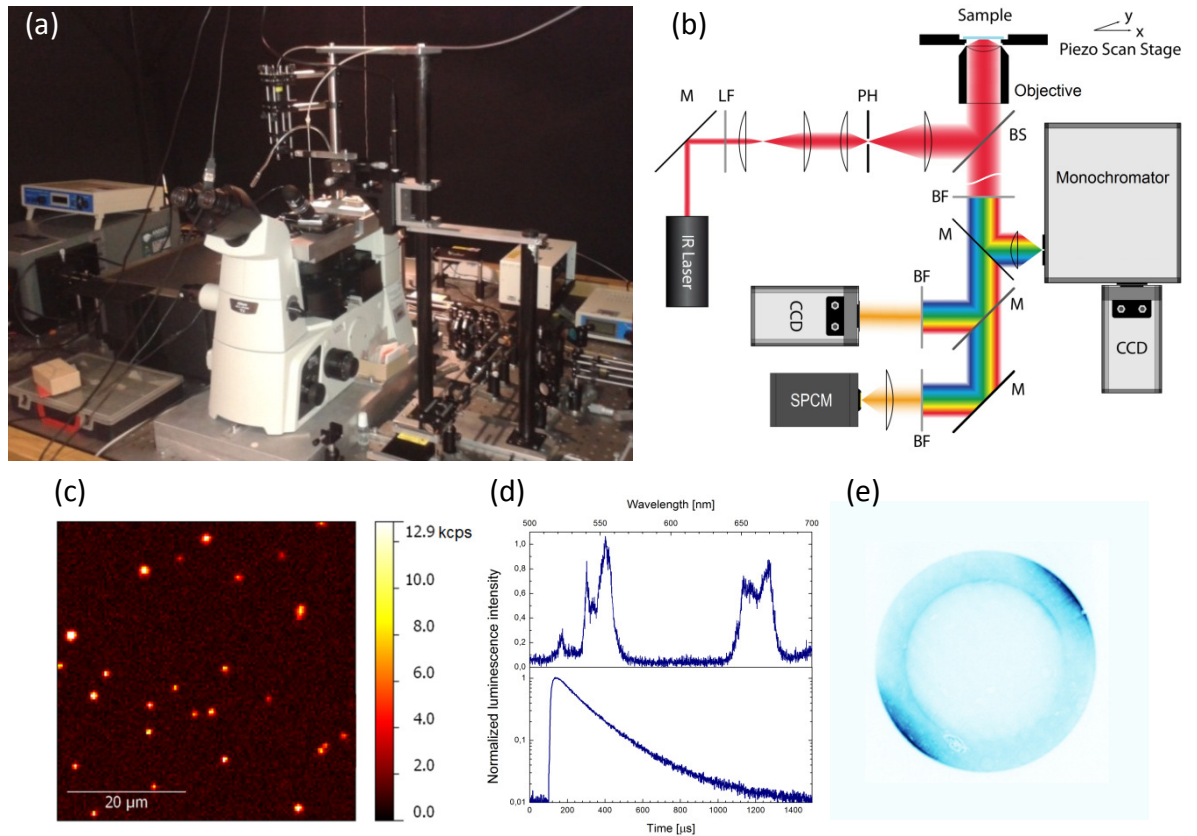
Fig. 5. (a) Photography of the confocal luminescence microscope built in the Institute of Physcis NCU. (b) Schematic of the experimental setup, where: BS – beam splitter, PH – pinhole, BF – band pass filter, LF – laser filter, M – mirror, λ_{exc}=980 nm, λ_{det1}=540/40 nm, λ_{det2}=650/30 nm. Exemplary data demonstrate: (c) red luminescence intensity map of single nanocrystals, (d) emission spectrum together with luminescence transient acquired from a single nanocrystal, (e) radiation pattern of a single hybrid nanostructure (nanocrystal+nanowire) recorded in the Fourier space.

(Perkin Elmer, SPCM-AQR-14). Filters dedicated to particular emission lines are mounted directly in front of the detector. The single photon counting unit can be connected either to a counter card (National Instruments, PCI-6232) for photoluminescence imaging, or to the multiscaler card (Becker&Hickl, MSA-300) for time-resolved analysis of the emission. Radiation pattern of luminescence can be projected directly on a CCD chip (Andor, iDus) that allows angular-depended analysis of the emission. Alternatively, emitted light can propagate toward a monochromator (Andor, Shamrock 500i), equipped with EMCCD camera (Andor, Newton) for spectral analysis. The whole setup is controlled by a dedicated software programmed in LabVIEW.

Besides the basic functionality mentioned above, each microscope setup has been carefully optimized to carry out advanced measurements. Among them FLIM (*Fluorescence Lifetime Imaging Microscopy*), BFP (*Back Focal Plane*) imaging and TENOM (*Tip-Enhanced Near-field Optical Microscopy*) should be mentioned. Each of these techniques was developed and adapted to unique spectra and time-resolved characteristics of α-NaYF$_4$:Er^{3+}/Yb^{3+} nanocrystals. Consequently, using professional and specialized experimental equipment, it was possible to acquire high quality, unique experimental data, which enabled to describe qualitatively and quantitatively up-conversion processes that occur in plasmonic hybrid nanostructures.

10

In the following part of description, the most important and interesting results have been presented and briefly discussed. The focused of this description is the optical properties of plasmonic hybrid nanostructures, consisting of α-NaYF$_4$:Er^{3+}/Yb^{3+} nanocrystals coupled with metallic nanoparticles of different types. First, we studied the up-conversion phenomenon occurring in a single nanocrystal interacting with a gold nano-tip. The influence of the distance between nanocrystals and the tip on the efficiency of absorption and emission processes is discussed. We also described a special role of Yb^{3+} in metal-enhanced absorption and migration of the energy within a single nanocrystal. In the next step, gold spherical nanoparticles of diameter about 30 nm have been used to prepare a hybrid system, where MEF processes show spectrally-dependent distribution of the enhancement factor. I has been shown, that single nanocrystals feature enhanced intensity of one emission line (red luminescence), whereas the intensity of the other emission line is strongly quenched. Afterwards, the optical properties of hybrid nanostructures consisting of elongated metallic nanoparticles (i.e. silver nanowires) are discussed. The role of propagating plasmonic excitations in absorption and emission processes has been investigated and discussed. We have shown, that silver nanowires sensitize the hybrid nanostructure for polarized light and participate in radiative relaxation of the nanocrystals. Additionally, influence of geometry of hybrid nanostructure on efficiency of MEF processes, that occur for nanocrystals positioned in different parts of the nanowire, has been examined and presented. In the last part of this study, we discuss a unique hybrid nanostructure, which has been specially optimized to show contribution of SPPs in the excitation and emission, in small population of nanocrystals. For this purpose, we developed a unique method, which allows for very precise deposition of extremely small volumes (femtoliters) of nanocrystals only on one end of a nanowire. It has been demonstrated that activation of the up-conversion luminescence can be realized exclusively by plasmon polaritons, excluding participation of the photons. It has also been shown that spectrally and time-resolved spectroscopic characterization of single emitters (nanocrystals) can be realized exclusively via SPPs.

IV.c.4. <u>Experimental results</u>

[B.P1] *„Tip enhancement of upconversion photoluminescence from rare earth ion doped nanocrystals",*
ACS Nano, 2015, Volume: 9, Issue: 4, Pages: 3617-3626

The physical properties of plasmonic hybrid nanostructures based on up-converting nanocrystals, differ from well known systems based on i.e. single molecules [19]. Nanocrystals (including α-NaYF$_4$:Er^{3+}/Yb^{3+}) are relatively large, often comparable with diameters of some metallic nanoparticles. Additionally, optically active ions (i.e. Er^{3+}) are distributed throughout the entire volume of the nanocrystal, and feature different distance to the surface. Therefore, understanding the influence of the distance between the nanocrystal and metallic nanoparticle on efficiency of the up-conversion process is an interesting and important problem.

In the experiment we used fluorescence microscope, presented in the previous section (IV.c.3). The microscope has been integrated with a specialized AFM head (shear-force type) [33], and adapted to luminescence properties of anti-Stokes materials. Eventually, the microscope achieved functionality of near-field optical microscope TENOM [34]. It allows optical (luminescence) imaging of single nanostructures with high spatial resolution (20-30 nm). At the same time, the microscope has functionality of classical confocal microscope and AFM.

One of the most important part of the TENOM microscope is a metallic tip. The tip is responsible for modification of the radiative processes of nearby emitters. Several dozens of gold tips have been prepared using electro-chemical etching technique. Diameter of the tip was typically about 20-30 nm, what was each time verified using SEM microscope. Such gold tips are optically active in a broad spectral range, from visible to infrared part of the spectrum [32]. Therefore, they can operate in the same spectral range as Er^{3+} doped nanocrystals. TENOM microscope makes it possible to position the gold tip only few nanometers from the surface, coaxially with the objective, which is localized under the sample, as presented in Fig. 6a. If the luminescence enhancement in MEF process occurs, it gives dominant contribution to the observed emission. Since MEF can be observed only near to the tip, TENOM allows optical imaging beyond the diffraction limit of light, and is limited only by a diameter of the tip.

Investigated sample consists of single α-NaYF$_4$:Er^{3+}/Yb^{3+} nanocrystals, deposited (spin-coated) on a glass coverslip. Topography of the sample, realized using shear-force AFM head, proves the presence of single nanocrystal, whose height is about 40 nm and diameter is about about 120 nm, as presented in Fig. 6b. Single nanocrystal visualized optically by TENOM microscope is presented in Fig. 6c. Very intense red luminescence (red and orange pseudo-color) – which dominates broad confocal signal (turquoise pseudo-color) – well correlates with AFM topography. It proves that luminescence enhancement appears only when tip is positioned very close to the nanocrystal.
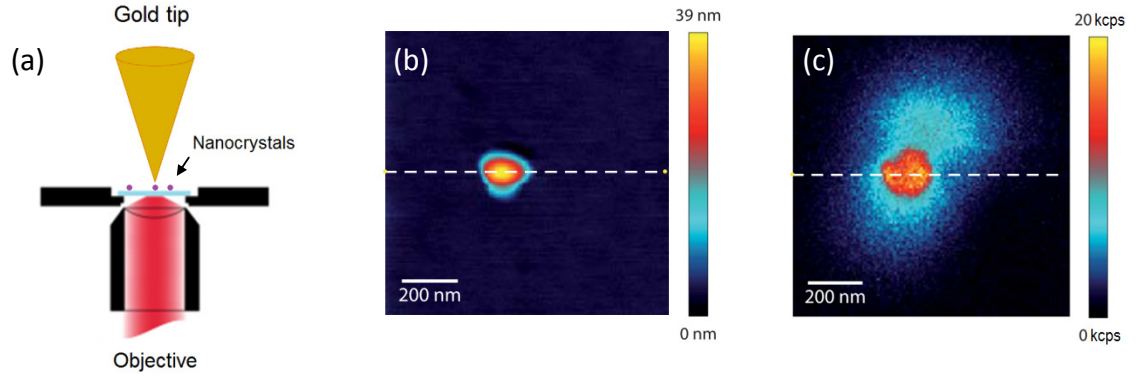
Fig. 6. (a) General concept of the experiment performed using TENOM microscope. Single α-NaYF$_4$:Er^{3+}/Yb^{3+} nanocrystal visualized by (b) AFM and (c) TENOM microscope (λ$_{det}$=650 nm, λ$_{exc}$=980 nm) [35].

Single nanocrystal interacting with gold tip can be considered as a model plasmonic hybrid nanostructure. High spatial resolution of tip positioning makes it possible to prepare a hybrid nanostructure of almost any distance between the particles. In this experiment we measured the emission spectrum of a single nanocrystal localized near (10-15 nm) and far from the tip. We observed increased intensity of the emission for both green and red emissions of the nanocrystal. Additionally, we measured luminescence transients for both emission lines. In the presence of the tip, transients feature bi-exponential decays, whereas reference decay profiles have mono-exponential character (Fig. 7a). The additional fast components, indicate that radiative emission rates increase in the presence of the tip. The slow components, which correspond to the reference measurements, demonstrate that not all Er^{3+} ions efficiently interact with the tip. Such a behavior is expected since dopant ions occupy different positions in relatively big nanocrystal.
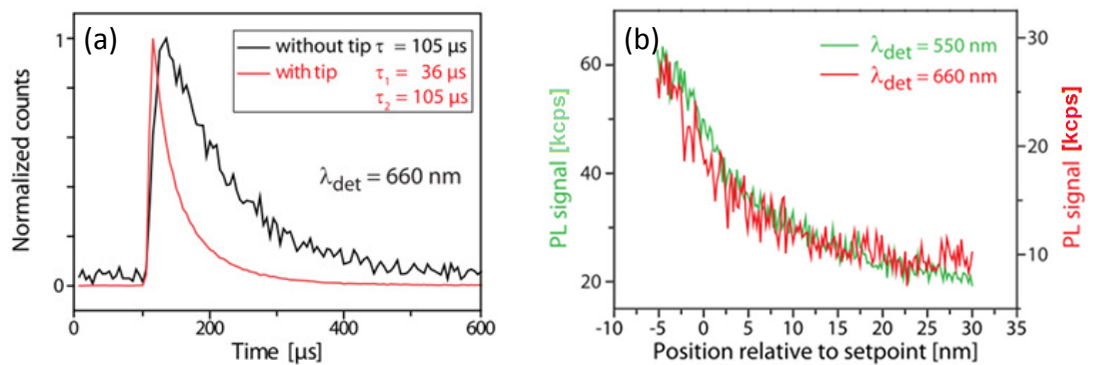

Fig. 7. (a) Luminescence transients of red emission taken from single α-NaYF$_4$:Er^{3+}/Yb^{3+} nanocrystal in the presence (red line) and in the absence (black line) of tip. (b) Approach curves, illustrate the luminescence (green and red) intensity measured versus decreasing distance between tip and the nanocrystal [35].

13

Very interesting data has been collected in a "tip-approach" experiment. In this case, the luminescence intensity is acquired versus distance between tip and nanocrystal. The approach curve makes it possible to determine the role of distance in the anti-Stokes metal-enhanced luminescence process (Fig. 7b). The reference signal (taken with fully retracted tip) was about 20 kcps for green and 10 kcps for red emission. Afterwards, the emission intensity collected with tip features about 60 kcps for green and 30 kcps for red emission. This observation allows to estimate luminescence enhancement factor to be about 3. Interestingly, in contrast to single molecule experiment, nanocrystal featured no luminescence quenching for the tip in contact with the nanocrystal. This proves that due to relatively large diameter of the nanocrystal, only small population of Er^{3+} ions remains in close contact with the tip, and therefore, can be quenched. At the same time, more distant ions can still emit or even experience some luminescence enhancement. We conclude that tip-induced luminescence quenching (previously observed for single molecules) does not exist for α-NaYF$_4$:Er^{3+}/Yb^{3+} nanocrystals or cannot dominate the emission process of the whole nanocrystal.

One should realize that confocal image (the reference one) consists of collective emission of all Er^{3+} ions in the nanocrystal. However, tip enhanced luminescence can be attributed to small population of the ions, localized very close to the tip. Regarding diameter of the tip and approximate depth of penetration of the nanocrystal by EM field (localized around the nanocrystal), actual luminescence enhancement factor should be about several hundred! So extreme enhancement factor cannot be explained only by metal enhanced emission rate. We proved that significant contribution comes from very efficient absorption of light, which occurs in the vicinity of the tip. Additionally, very efficient energy migration between high population of Yb^{3+} ions (20 mol%) distribute the energy within the nanocrystal. Therefore, despite the fact that only small population of Er^{3+} ions can interact with the tip, effective absorption of the excitation energy within a hybrid plasmonic nanostructure can be very efficient.

In this work we discussed metal enhanced anti-Stokes luminescence of single α-NaYF$_4$:Er^{3+}/Yb^{3+} nanocrystal induced by a gold tip. By changing position of the tip we investigated influence of distance between these particles on the efficiency of MEF process. The role of absorption and energy migration within single nanocrystal has been discussed.

[B.P2] *„Spectral Selectivity of Plasmonic Interactions between Individual Up-Converting Nanocrystals and Spherical Gold Nanoparticles", Materials, 2017, Volume: 10, Pages: 905-915*

Efficiency of interaction between nanocrystal and metallic nanoparticle, that occurs within plasmonic hybrid nanostructure, depends on their mutual spectral relations. Already studied plasmonic hybrid nanostructures, mostly based on molecules and quantum dots, feature rather broad absorption/emission bands. Therefore, precise spectral tuning and optimizing of their spectral relations was usually ineffective. In the next publication we have shown that in the presence of suitably adjusted metallic nanoparticle, emission rates of selected radiative transitions in the rare earths doped nanocrystal can be modified and controlled individually. In particular case of Er^{3+}, infrared excitation at 980 nm activates two relatively narrow emission lines (green and red),

which are spectrally isolated from the excitation wavelength. Additionally, due to two-photon anti-Stokes excitation, excited radiative states $^2H_{11/2}$+$^4S_{3/2}$ and $^4F_{9/2}$ are populated independently, utilizing partly separated excitation channels described in details in section IV.c.2. By using dedicated metallic nanoparticles we have shown that emission rates of green and red luminescence can be controlled and modified independently.

In the experiment we used experimental setup described in section IV.c.3. It features typical functionality of luminescence confocal microscope, including photoluminescence imaging and spectral analysis of individual nanostructures. Additionally, it has been upgraded and properly programmed to enable advanced time-resolved imaging techniques, including FLIM. The general concept of FLIM experiment is as follows. For each position on the sample, both PL intensity and emission transients are collected. In the next step, both emission intensity and decay constant are used to plot spatial distribution of the luminescence dynamics. Because of relatively slow $f{\rightarrow}f$ emission and to distinguish from biological application, we will call this technique µs-FLIM.

In the experiment we investigated two types of samples. The first one (reference) consists of α-NaYF$_4$:Er^{3+}/Yb^{3+} nanocrystals, spin-coated on a glass coverslip. The second sample (hybrid) consists of nanocrystals, deposited on a glass substrate previously coated by a thin layer of gold nanoparticles. We used spherical gold nanoparticles with a radius of about 15 nm. They feature only one, relatively narrow absorption band, positioned at 530 nm. Therefore, within the hybrid nanostructure, only one emission line (green) of the nanocrystals spectrally overlaps with extinction of the gold nanoparticles. The second (red) emission line is localized near the minimum of the extinction. Therefore, in the prepared hybrid nanostructure, emission rates of two luminescence transitions can be modified individually and independently.

In the first step we visualized spatial distribution of photoluminescence intensity of the reference sample. Both PL maps – acquired for green and red emission of α-NaYF$_4$:Er^{3+}/Yb^{3+} nanocrystals under 980 nm excitation – are very homogeneous. The nanocrystals feature average intensity of the emission about 25-30 kcps for both emission lines. Next, the same part of the reference sample has been analyzed using µs-FLIM technique. The average nanocrystal decay time for the considered area was about 75 µs for green and 140 µs for red emission. Additionally, both PL and µs-FLIM maps show perfect spatial correspondence. In other words, every single nanocrystal contributes to both photoluminescence and µs-FLIM map.

In the next step we analyzed the hybrid sample. This time, PL intensity maps (acquired for both emissions) are qualitatively different. They indicate existence of two populations of nanocrystals, interacting differently with gold nanoparticles. One group of the nanocrystals shows both emissions, and intensity of the red luminescence slightly increased compared to the reference. On the other hand, the second group of the nanocrystals does not show green emission at all. At the same time, intensity of red emission is strongly enhanced, as presented in Fig. 8ab. In the µs-FLIM experiment we observed shortening of the luminescence decay time down to 60 and 100 µs, for green and red emission, respectively (Fig. 8cd). Interestingly, the second population of the nanocrystals (that shows no green luminescence) features extremely short decay times of the red emission, below 30 µs.
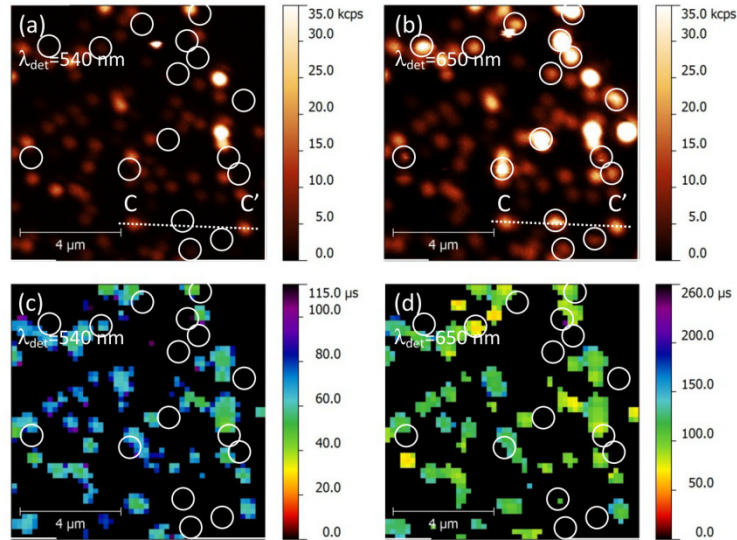
Fig. 8. Photoluminescence intensity map of hybrid sample, acquired for (a) green and (b) red emission of the nanocrystals. The correspondence µs-FLIM maps are presented in section (c) and (d), respectively [31]. The second population of nanocrystals, that show no green emission and very fast red luminescence are marked with white circles.

To understand the twofold behavior of the nanocrystals within the hybrid nanostructure, we considered a simple theoretical model. It is based on elements of Mie theory [36][37] and classical electrodynamical model of interaction between a single emitter and a metallic nanoparticle [38][39]. Considered model takes into account presence of a single dipolar emitter, positioned 5, 15 and 30 nm from the surface of the gold nanosphere of 30 nm in diameter, and oriented parallel or perpendicular to the surface of the nanoparticle.

Theoretical analysis shows that emission rate enhancement (within such a plasmonic hybrid nanostructure) can be observed in a broad spectral range, from 400 to 700 nm. The enhancement factor grows rapidly with decreasing distance between the emitter and the sphere. The maximum rate enhancement is achieved for d=5 nm (parallel orientation) and the emission wavelength near 510 nm. However, in the real system, competition between emission rate enhancement and luminescence quenching (i.e. absorbance of nanoparticle) should be taken into account. The calculated quantum efficiency factor indicates that luminescence enhancement occurs in a limited spectral range, which is typically spectrally red-shifted with respect to the maximum extinction of metallic nanoparticles [19].

Spectral distribution of quantum efficiency calculated for d=30 nm, is consistent with experimental results assigned to the first group of nanocrystals. Calculations confirm presence of two emission lines (green and red) and predict slightly increased emission rates (reduction of decay times). Properties of the second group of the nanocrystals can be also described within the same theoretical model, however, much shorter distance must be considered. Calculation performed for d=5 nm show very efficient quenching of the green emission, which is attributed to the nonradiative energy transfer from nanocrystal to gold nanoparticles. At the same time, noticeable increase of quantum efficiency is expected for longer emission wavelengths (above 650 nm), and accompanied by distinctly reduced luminescence decay constants. According to the calculations,

16

enhancement of the emission intensity is especially high, if we assume some dispersion of nanoparticles diameters (15 nm < r < 30 nm) and perpendicular orientation of the dipole.

In this work we demonstrated that enhancement of the luminescence intensity, observed within plasmonic hybrid nanostructures, strongly depends on mutual spectral relation between emitter and metallic nanoparticle. We have shown that after appropriate optimization it is possible to observe at the same time enhancement and quenching of two different emission lines within one nanostructure. We demonstrated that those processes depend on the distance between a dipolar emitter and metallic nanoparticles, as well as relative orientation of the dipole.

[B.P3] *„Silver nanowires as receiving-radiating nanoantennas in plasmon-enhanced up-conversion processes",* Nanoscale, 2015, Volume: 7, Issue: 4, Pages: 1479-1484

Among modern metallic nanostructures, elongated nanoparticles form a distinctly different class of materials. Silver nanowires – for instance – can support surface plasmon polaritons, which can propagate on metal-dielectric interface. SPPs can be activated by light and transport the excitation energy along the nanowire. In the plasmonic hybrid nanostructure, besides already discussed luminescence enhancement, additional processes involving propagation can be observed. For example, SPPs can participate in excitation and emission processes of nearby nanocrystals. Due to low symmetry of the nanowires, polariton-mediated processes depend on geometry of the sample and polarization of the excitation beam.

In the experiment we used the microscope setup presented in the previous sections. It allows PL imaging, as well as spectral and time-resolved analysis of single nanostructures, including μs-FLIM. In this work, however, polarization of the laser beam was controlled precisely. We used high quality linear polarized together with a quarter-wave plate to freely rotate polarization vector around the beam axis. Also the spatial distribution of EM field in the excitation beam was carefully controlled. Typically we used a Gaussian mode TEM_{00}. However, the fundamental Gaussian mode focused by a high numerical aperture objective has rather complex character. If the incidental beam is polarized linearly, tightly focused beam features the same linear and transversal polarization. Additionally, a longitudinal component oriented along the propagation direction is observed [32].

The hybrid sample has been prepared in several steps by using spin-coating technique. First, water solution of silver nanowires was deposited on glass coverslip. Concentration of the colloid was optimized so as to obtain density of nanoparticles of a few nanowires (4-5 on average) per 100 μm^2. In the next step, colloidal solution of α-NaYF$_4$:Er^{3+}/Yb^{3+} nanocrystals dissolved in chloroform has been spin-coated on the substrate. Density of the colloid was about 1 mg/ml. It was optimized in such a manner that obtained density of the nanocrystal was quite high but still free of agglomeration.

The purpose of the first measurement was to localize silver nanowires on the substrate. To do this, we used confocal microscope operating in light scattering mode. By analyzing spatial distribution of scattered laser radiation we localized several silver nanowires, randomly arranged on the substrate, as presented in Fig. 9a. In the next step, the same part of the sample was visualized using PL imaging (Fig. 9b). Analyzing both maps we can conclude that intensity of the nanocrystals emission is on average 7 times higher (with respect to the reference) if they are localized near the silver nanowires.
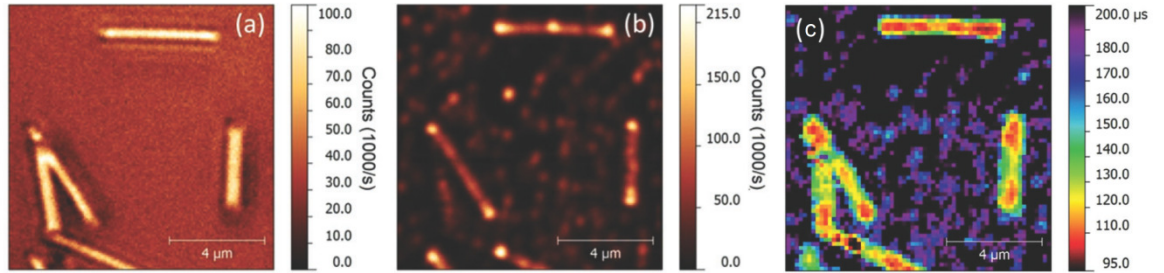

Fig. 9. (a) Light scattering map presents arrangement of silver nanowires on the sample. (b) PL intensity map (λ_{em}=650 nm) and (c) µs-FLIM map acquired for the same part of the sample [36].

Increase of the radiative emission rates, which can be observed in the vicinity of metallic nanoparticles, is one of the most crucial phenomenon that contributes to observed luminescence enhancement. In the next experiment we used µs-FLIM technique to analyze dynamics of luminescence in the plasmonic hybrid nanostructure. Exemplary µs-FLIM map, acquired over the same part of the sample, is presented in Fig. 9c. One can notice that red emission decay times, acquired for nanocrystals localized near silver nanowires (125 µs on average) are much shorter than the reference ones (175 µs on average). Decrease of the luminescence decay time is accompanied by increase of the luminescence intensity. Therefore, we conclude that Purcell effect has significant contribution to the observed luminescence enhancement.

In this research we also shown that for silver nanowires, increase of the luminescence intensity depends not only on distance between nanocrystal and nanoparticl,e but also on the position of particular nanocrystal (emitter) relative to the nanowire. Statistical analysis shows that the highest increase of the radiative emission rates is observed for nanocrystals localized close to the end of the nanowire. It means that in a such a position, interaction between the emitter and nanowire is the most efficient. This is due to large curvature of the nanowire surface, providing good matching between wavevector of the emitted radiation and the polariton [37].

Finally, we performed the experiment, where photoluminescence imaging of the hybrid nanostructure was realized using linearly polarized excitation (laser) beam. In this case, we always acquired two complementary PL maps, collected using two orthogonal linear polarizations. We observed that metal-induced increase of the luminescence intensity is the highest when excitation radiation is polarized linearly and parallel to the nanowire. The PL intensity contrast, estimated as the ratio of two polarization states, was about $3-4$. One should remember that rare earths doped nanocrystals feature no permanent dipole moment. At the same time, amount of the energy

18

absorbed by the nanowire depends on the polarization of incidental laser beam. Therefore, in this experiment we proved that silver nanowire behaves as optically active nanoantena, transferring the collected excitation energy directly to nanocrystals. Effective increase of the absorption efficiency, observed within plasmonic hybrid nanostructure, is related to much higher absorption cross section of the nanowire. Therefore (besides Purcell effect) effective increase of the absorption efficiency gives significant contribution to the overall luminescence enhancement phenomenon.

In this work we presented a microscopic picture illustrating metal enhanced luminescence phenomenon that takes place in a plasmonic hybrid nanostructure consisting of α-NaYF$_4$:Er^{3+}/Yb^{3+} nanocrystals and single silver nanowires. We demonstrated that increase of the radiative emission rates depends on spatial position of nanocrystals relative to the nanowire. We have shown that silver nanowires increase effective absorption efficiency and sensitize the nanostructure for polarization state of the excitation beam.

[B.P4] *„Radiation channels close to a plasmonic nanowire visualized by back focal plane imaging",* ACS Nano, 2013, Volume: 7, Issue: 11, Pages: 10257-10262

In the next publication we discussed the role of propagating plasmon polaritons in radiative dissipation of the energy by a plasmonic hybrid nanostructure. In the experiment we used the same microscope setup. However, it has been significantly upgraded by additional detection channel, designated for back focal plane detection in the Fourier space. We used additional, external lens for transformation of the real space image, and projection on a CCD chip [38]. Acquisition of valuable information, regarding angular distribution of the emitted radiation, required the use of objective featuring large numerical aperture (NA=1.4). The experiment has been performed using the same type of hybrid sample discussed in the paragraph [B.P3]. It consists of α-NaYF$_4$:Er^{3+}/Yb^{3+} nanocrystals coupled with single silver nanowires. Additionally, it has been investigated using AFM microscope, to receive topographic information, and determine precise location of single nanocrystals relative to the nanowire.

BFP measurement gives a lot of valuable information regarding angular distribution of the emitter radiation. In the case of a single molecule (single dipole), the image recorded in the Fourier space (radiation pattern) has a form of round map, typically of inhomogeneous distribution of the radiation intensity. Careful analysis of the radiation distribution – carried out individually for each emitter – allows to estimate exact orientation of the molecule during emission process [39]. Interestingly, radiation patterns can give crucial information regarding role of surface plasmon polaritons in the processes of distribution and reemission of the radiation within plasmonic hybrid nanostructures.

Exemplary PL intensity map of the nanocrystals localized in the vicinity of single silver nanowire is presented in Fig. 10a. The nanostructure has been investigated using BFP technique, by acquiring red luminescence of the nanocrystals in the Fourier space. Recorded radiation patterns are presented in Fig. 10bcd and differ in the excitation geometry, with the laser spot focused precisely on (b) lower-left end of the nanowire, (c) middle of the nanowire and (d) upper-right end of the nanowire.
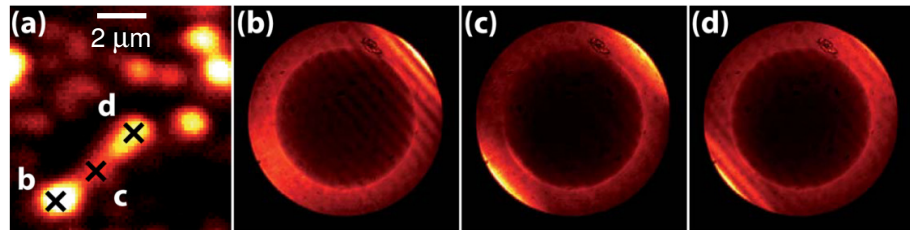

Fig. 10. (a) Exemplary PL intensity map illustrating emission of the nanocrystals positioned in the vicinity of single silver nanowire. Radiation patterns were collected at 650 nm under 980 nm laser excitation focused on (b) lower-left end, (c) middle, and (d) upper-right end of the nanowire [40].

BFP radiation patterns, recorded for considered hybrid nanostructures, feature quite complex character. First of all, they consist of a bright and regular rim. Due to random orientation of the nanocrystals and a lot of dopant ions, information of orientation of particular ions is averaged. Therefore, the rim can be attributed to direct emission from the nanocrystals. Additionally, each pattern contains several intense fringes, which are oriented perpendicularly to the axis of symmetry of the nanowire.

Interestingly, presence of bright fringes directly proves contribution of SPPs in the emission process. Nanocrystals, however, can emit the energy directly to free space or transfer it nonradiatively to the nanowire. In the latter case, relaxing ions launch polaritons, which receive the energy and transport it along the metal-dielectric interface (along the nanowire). During this process, the energy is reemitted under leakage radiation, contributing to the collected BFP radiation patterns [41]. Leakage radiation gives important information regarding geometry of the metallic nanostructure, its orientation, as well as other spatial limitations. Additionally, depending on the excitation point, observed fringes differ in distribution and numbers. When the considered plasmonic hybrid nanostructure is excited by a laser spot focused on lower-left end of the nanowire (case *b*), activated polariton propagates towards upper-right end, contributing to the fringes presented in Fig. 10b. Symmetrical situation occurs when upper-right end of the nanowires is being excited. On the other hand, nanostructure excited by a laser focused in the middle of the nanowire, shows polaritons propagating towards two directions, contributing to the fringes visible in Fig. 10c.

Careful analysis of BFP patterns allows to estimate direction and magnitude of the wave vector of propagating polaritons. Our experiment has shown that in the considered plasmonic hybrid nanostructure, polaritons do not propagate strictly on a metal-dielectric or metal-air interface. On the contrary, our results demonstrate that polaritons hybridize, combining features of these two materials. We directly proved that silver nanowires do not participate only in the absorption processes, but significantly contribute to distribution and reemission of the energy.

Eventually, by comparing intensity of emission contained in a rim and in fringes, one can estimate relative energy distribution between radiative deexcitation channels available for the nanocrystals.

In this work we directly proved that silver nanowires participate in distribution and reemission of the energy converted by α-NaYF$_4$:Er^{3+}/Yb^{3+} nanocrystals. BFP analysis demonstrates that propagation direction of polariton strictly depends on sample geometry and excitation point. We also estimated magnitude of wave vector of surface plasmon polaritons and contribution of polaritons in radiative processes of deexcitation of the nanocrystals.

[B.P5] *„Remote activation and detection of up-converted luminescence via surface plasmon polaritons propagating in a silver nanowire",* Nanoscale, 2018, Volume: 10, Issue: 26, Pages: 12841-12847

The role of metallic nanoparticles in the anti-Stokes luminescence processes (attributed to the α-NaYF$_4$:Er^{3+}/Yb^{3+} nanocrystals) can have complex character. In optimal conditions, their presence can increase efficiency of absorption and radiative emission rates of the nanocrystals. Additionally, silver nanowires can sensitize the plasmonic hybrid nanostructure to polarization state of incidental beam, and can participate in excitation processes. Due to BFP imaging we shown that surface plasmon polaritons can transport and reemit the energy up-converted by nanocrystals. In the last experiment, being original summary of the whole presented research project, we took advantage of obtained knowledge and experience to perform an experiment, in which propagating surface plasmon polaritons allow remote control of the optical properties of up-converting nanocrystals.

We put in a lot of effort to prepare a sample of strictly controlled geometry and functionality. In contrast to already presented data, where distribution of nanocrystals and nanowires was rather random, in this case position of nanocrystals relative to the nanowire was strictly defined. Self-prepared and then investigated sample consists of a single silver nanowire with diameter of about 200 nm and lengths of 18 μm. On one (upper) end of the nanowire we deposited very small population of the nanocrystals, what can be seen in Fig. 11a. To do this, we used original technique regularly applied for *in vitro* procedures [42]. Small amount of colloidal nanocrystals (femtoliters) was transferred on the surface using a glass pipette with inner diameter of about 500 nm. Position of the pipette was controlled very precisely using piezoelectric manipulator, operating in 3D. The whole instrument has been mounted on top of the confocal microscope, allowing real-time control of the sample preparation process.
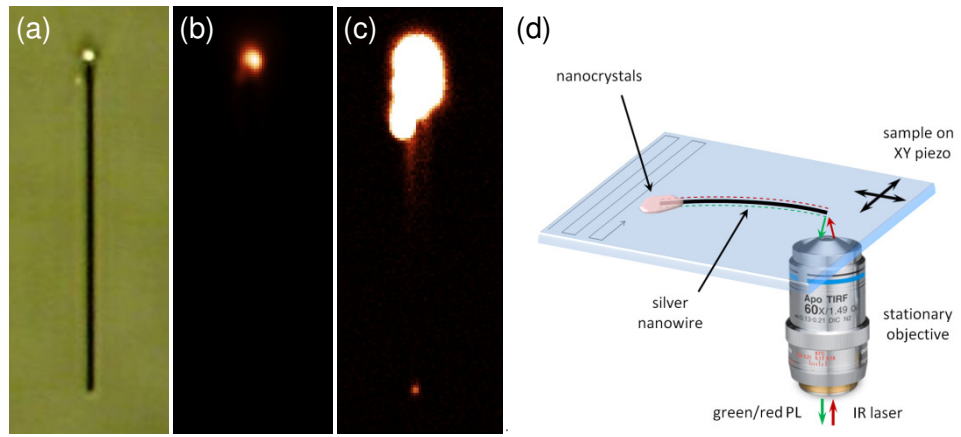
Fig. 11. *Microscopic image of a single silver nanowire, decorated by small population of nanocrystals, visualized by (a) transmission and (b) PL microscopy (λ_{det}=650 nm). (c) PL map demonstrating emission of light from free (lower) end of the nanowire. (d) Experimental configuration used to investigate polariton-mediated excitation and emission processes [42].*

In the experiment we used confocal fluorescence microscope described in details in the previous paragraphs. We visualized prepared nanostructure using photoluminescence imaging mode. Acquired PL intensity map is presented in Fig. 11b. It proves that small population of the emitters (nanocrystals) is localized exclusively near the upper end of the nanowire. Also SEM measurements do not show any other nanocrystals near the nanowire, but only these on nanowire end. In the first step we investigated emission transients of both emissions. Estimated decay times are much shorter than we observed for the reference sample. It proves that deposited nanocrystals interact with the nanowire quite efficiently.

In the next step we visualized lower end of the nanowire. This end is physically free of the nanocrystals. Nevertheless, using full available excitation power (about 20 mW) we can observe luminescence signal, what is presented in Fig. 11c. The physical configuration leading to this observation is presented in Fig. 11d. The laser spot focused on free end of the nanowire launches polaritons, which can propagate towards opposite end. Polarization resolved analysis shows that this process is most efficient when excitation light is polarized linearly, along the nanowire. Polaritons reaching upper end interact with nanocrystals and activate up-conversion process. Due to sequential, two-step absorption of the energy excited states of Er^{3+} are being excited. Now, there are two scenarios of the deexcitation process, which can be realized either due to radiative emission of light (local), or due to polaritons activated by excited nanocrystals. Such polaritons propagate back to the lower end, where the energy is released radiatively to open space [38].

Spectral analysis of the radiation emitted by the lower end of the nanowire shows a spectrum, which consists of two lines peaking at 540 and 650 nm, which can be assigned to the luminescence emission of Er^{3+} ions. This observation proves that nanocrystals are indeed a source of the emission in considered nanostructure. Additionally, we observed that in the process, green luminescence is quenched by the nanowire much more that the red one. We have found two reasons that can contribute to this effect. First of all, attenuation of radiation by a silver nanowire increases with rising energy of polariton. Such a behavior can be deduced from the absorption

spectrum of colloidal nanowires [43]. Secondly, as it was already discussed, metal-induced enhancement of the luminescence is spectrally selective. The enhancement factor reaches maximum for emission lines red-shifted with respect to the maxima of extinction of nanoparticles [31][44]. These two effects spectrally modify the nanostructure in such a manner that red luminescence dominates intensity of green emission.

More information can be obtained with time-resolved analysis of the emitted radiation. First, it should be noticed that silver nanowires do not emit at all under 1 µs long (pulsed) laser excitation at 980 nm. Furthermore, propagation time of polaritons can be assumed to be infinitively short with respect to the luminescence decay times observed in Er^{3+}. In the considered sample, luminescence transients acquired from the lower end at 540 and 650 nm feature decay constants of about 30 and 110 µs, respectively. Interestingly, life times estimated directly for nanocrystals localized on upper end of the nanowire are longer, and equal about 60 and 130 µs. Therefore, we conclude that geometry of the sample determines effective population of the nanocrystals contributing to the acquired transients. For direct laser illumination, excitation spot (400-500 nm in diameter) excites large population of the nanocrystals, localized both close and far from the nanowire. Therefore, due to metal-emitter distance variations, rate enhancement factors, as well as decay times can fluctuate, and in the experiment averaged life time is collected. In the situation when polaritons remotely activate nanocrystals, population of the nanocrystals is strongly limited to nanocrystals positioned very close to the nanowire. These nanocrystals feature very high (and similar) rate enhancement factor and very short life time of the luminescence

In the present experiment we used propagating surface plasmon polaritons remotely control remotely (and fully bi-directional) small population of up-converting nanocrystals, localized on one end of a single silver nanowire. Our demonstration exceeds results presented by other groups, where only one-directional polariton mediated processes have been observed. These qualitatively new results demonstrate quite new functionality of such a plasmonic nanostructure. We have defined new class of non-local optical processes (occurring in hybrid nanostructures), which allows to control luminescence processes or other (i.e. chemical) reactions at the nanoscale. On the other hand, SPPs can participate in spectrally and time-resolved characterization of single emitters. These results may have significant impact on integrated nanosensorics and biomedical/diagnostics applications.

IV.c.5. <u>Summary</u>

Presented scientific achievement is an original and important contribution to understanding physical processes that occur within plasmonic hybrid nanostructures. Discussed publications present new experimental results regarding up-conversion processes taking place in rare earths doped nanostructures localized close to metallic nanoparticles. This research complements and significantly expands current state of knowledge with innovative and high quality experimental results.

One of the most significant achievement is detailed description of the optical properties of a single α-NaYF$_4$:Er^{3+}/Yb^{3+} nanocrystal localized in the vicinity of metallic nanoparticles. Plasmon enhanced up-conversion process has been observed and studied in details using tip-enhanced near field optical microscope technique, TENOM. The microscope has been rebuilt, optimized, and adopted in order to make it possible to investigate up-converting nanomaterials. In this research it has been shown that metal enhanced up-converted luminescence can be efficiently and very precisely activated within single a nanocrystal that is much larger than effective diameter of the metallic tip (or nanoparticle). We have also shown that such a hybrid nanostructure is less sensitive to emission quenching (caused by too small distance between nanocrystal and tip) than already studied systems involving single molecules. We demonstrated that efficient, metal-enhanced absorption (in a single nanocrystal) is realized mostly due to nonradiative energy transfer between Yb^{3+} ions. In the next step, we used unique luminescence properties of up-conversion nanocrystals to demonstrate spectrally selective enhancement of the luminescence. For this research, we used carefully optimized gold spherical nanoparticles to optimize the system in such a manner that one (red) emission was enhanced, whereas at the same time the second (green) emission was strongly quenched. It was the first demonstration of such a selective plasmonic effect within single nanoemitter. This result can be of particular interest for e.g. advance biomedical imaging or microscopic analytical analysis.

A lot of new information was provided by a series of microscopic experiments performed on plasmonic hybrid nanostructures consisting of elongated metallic nanoparticles, especially silver nanowires. Due to new experimental techniques like μs-FLIM and BFP imaging, we investigated influence of the geometry of elongated metallic nanoparticle on the efficiency of MEF process. We investigated the role of SPPs in absorption and emission processes that take place within the hybrid nanostructure. Eventually, we have shown that propagating plasmon polaritons (which are activated by light) can be exploited for bi-directional, remote control of small population of the nanocrystals localized on one end of the nanowire. We demonstrated that propagating polaritons can mediate in spectrally and time-resolved analysis performed for such a nanostructure. Moreover, in contrast to already known light-controlled experiments, we have shown that up-conversion process involving ETU mechanisms can be realized exclusively by polaritons. In other words, we proved that in some cases photons can be eliminated from the experiment carried out at strictly optical frequencies.

The presented scientific achievement has a basic research character. Nevertheless, due to observation of new and unique effects, it suggests possible innovative applications. From this point of view, especially interesting are plasmonic hybrid nanostructures featuring non-local effects. We have shown that besides luminescence enhancement in MEF process, propagating polaritons effectively transport the energy within the hybrid nanostructure. Importantly, this process is undisturbed by diffraction, and can effectively connect macroscopic optical elements (apparatus) with single nanoemitters. Single silver nanowire can be therefore considered as alternative development path of optoelectronic devices, allowing further miniaturization and potential applications in controlling physical, chemical and biological processes at the nanoscale.

The potential of nonlocal plasmonic/optical processes research has been appreciated by the Experts of National Science Centre of Poland. Thanks to financial support obtained within the SONATA BIS 7 program, I received the opportunity to establish my research group and carry out further research on polariton mediated, non-local processes in plasmonic hybrid nanostructures.
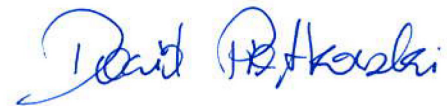
IV.c.6. **References**

[1] W.E. Moerner, L. Kador, Optical detection and spectroscopy of single molecules in a solid, Phys. Rev. Lett. 62 (1989) 2535–2538. doi:10.1103/PhysRevLett.62.2535.

[2] D.G. Zhang, X.-C. Yuan, A. Bouhelier, P. Wang, H. Ming, Excitation of surface plasmon polaritons guided mode by Rhodamine B molecules doped in a PMMA stripe, Opt. Lett. 35 (2010) 408–410. doi:10.1364/OL.35.000408.

[3] Y. Fu, J. Zhang, J.R. Lakowicz, Metal-Enhanced Fluorescence of Single Green Fluorescent Protein (GFP), Biochem. Biophys. Res. Commun. 376 (2008) 712–717. doi:10.1016/j.bbrc.2008.09.062.

[4] H. Wei, D. Ratchford, X. (Elaine) Li, H. Xu, C.-K. Shih, Propagating Surface Plasmon Induced Photon Emission from Quantum Dots, Nano Lett. 9 (2009) 4168–4171. doi:10.1021/nl9023897.

[5] W. Feng, L.-D. Sun, C.-H. Yan, Ag nanowires enhanced upconversion emission of NaYF4:Yb,Er nanocrystals via a direct assembly method, Chem. Commun. (2009) 4393–4395. doi:10.1039/B909164E.

[6] J. Grzelak, K. Ciszak, M. Nyk, S. Mackowski, D. Piatkowski, Extending light-harvesting of poly(3-hexylthiophene) through efficient energy transfer from infra-red absorbing nanocrystals: Single nanoparticle study, Appl. Phys. Lett. 105 (2014) 163114. doi:10.1063/1.4900488.

[7] B. Krajnik, N. Czechowski, K. Ciszak, D. Piatkowski, S. Mackowski, T.H.P. Brotosudarmo, H. Scheer, S. Pichler, W. Heiss, Plasmon-enhanced fluorescence in heterochlorophyllous peridinin-chlorophyll-protein photosynthetic complex, Opt. Mater. 34 (2012) 2076–2079. doi:10.1016/j.optmat.2012.04.015.

[8] V. Biju, Chemical modifications and bioconjugate reactions of nanomaterials for sensing, imaging, drug delivery and therapy, Chem. Soc. Rev. (2013). doi:10.1039/C3CS60273G.

[9] S. Schietinger, T. Aichele, H.-Q. Wang, T. Nann, O. Benson, Plasmon-Enhanced Upconversion in Single NaYF4:Yb3+/Er3+ Codoped Nanocrystals, Nano Lett. 10 (2010) 134–138. doi:10.1021/nl903046r.

[10] J.R. Lakowicz, Principles of Fluorescence Spectroscopy, 3rd ed., Springer, 2006.

[11] S.A. Maier, Plasmonics: Fundamentals and Applications, 2007th ed., Springer, 2007.

[12] M. Olejnik, Biokoniugacja nanostruktur metalicznych z kompleksami fotosyntetycznymi, Rozprawa doktorska, Toruń, 2013.

[13] A. Dasgupta, D. Singh, S. Tandon, R.P.N. Tripathi, G.V. Pavan Kumar, Remote-excitation surface-enhanced Raman scattering with counter-propagating plasmons: silver nanowire-nanoparticle system, J. Nanophotonics. 8 (2013) 083899–083899. doi:10.1117/1.JNP.8.083899.

[14] W. Demtröder, Laser Spectroscopy: Basic Concepts and Instrumentation, Springer Science & Business Media, 2002.

[15] W. Deng, F. Xie, H.T.M.C.M. Baltar, E.M. Goldys, Metal-enhanced fluorescence in the life sciences: here, now and beyond, Phys. Chem. Chem. Phys. 15 (2013) 15695–15708. doi:10.1039/C3CP50206F.

[16] W. Barnes, Fluorescence near interfaces: The role of photonic mode density, J. Mod. Opt. 45 (1998) 661–699. doi:10.1080/09500349808230614.

[17] E.M. Purcell, Spontaneous Emission Probabilities at Radio Frequencies, Phys. Rev. 69 (1946) 681. doi:10.1103/PhysRev.69.674.2.

[18] J.R. Lakowicz, Radiative decay engineering: biophysical and biomedical applications, Anal. Biochem. 298 (2001) 1–24. doi:10.1006/abio.2001.5377.

[19] P. Bharadwaj, P. Anger, L. Novotny, Nanoplasmonic enhancement of single-molecule fluorescence, Nanotechnology. 18 (2007) 044017. doi:10.1088/0957-4484/18/4/044017.

[20] P. Anger, P. Bharadwaj, L. Novotny, Enhancement and quenching of single-molecule fluorescence, Phys. Rev. Lett. 96 (2006) 113002. doi:10.1103/PhysRevLett.96.113002.

[21] B.G. Wybourne, Spectroscopic properties of rare earths, Interscience Publishers, New York, 1965.

[22] G. Blasse, B.C. Grabmaier, Luminescent materials, Springer-Verlag, 1994.

[23] F. Auzel, Upconversion and Anti-Stokes Processes with f and d Ions in Solids, Chem. Rev. 104 (2004) 139–174. doi:10.1021/cr020357g.

[24] R. Scheps, Upconversion laser processes, Prog. Quantum Electron. 20 (1996) 271–358. doi:10.1016/0079-6727(95)00007-0.

[25] L. Li, C. Guo, S. Jiang, D.K. Agrawal, T. Li, Green up-conversion luminescence of Yb3+-Er3+ co-doped CaLa2ZnO5 for optically temperature sensing, RSC Adv. 4 (2014) 6391–6396. doi:10.1039/c3ra47264g.

[26] M. Nyk, R. Kumar, T.Y. Ohulchanskyy, E.J. Bergey, P.N. Prasad, High Contrast in Vitro and in Vivo Photoluminescence Bioimaging Using Near Infrared to Near Infrared Up-Conversion in Tm3+ and Yb3+ Doped Fluoride Nanophosphors, Nano Lett. 8 (2008) 3834–3838. doi:10.1021/nl802223f.

[27] T.A. Henderson, L.D. Morries, Near-infrared photonic energy penetration: can infrared phototherapy effectively reach the human brain?, Neuropsychiatr. Dis. Treat. 11 (2015) 2191–2208. doi:10.2147/NDT.S78182.

[28] D. Piątkowski, Simulation of the absorption spectrum of Nd3+ activated fluoroaluminate glass, J. Non-Cryst. Solids. 353 (2007) 1017–1022. doi:10.1016/j.jnoncrysol.2007.01.013.

[29] H.P. Paudel, L. Zhong, K. Bayat, M.F. Baroughi, S. Smith, C. Lin, C. Jiang, M.T. Berry, P.S. May, Enhancement of Near-Infrared-to-Visible Upconversion Luminescence Using Engineered Plasmonic Gold Surfaces, J. Phys. Chem. C. 115 (2011) 19028–19036. doi:10.1021/jp206053f.

[30] D. Piatkowski, S. Mackowski, Excited state absorption in glasses activated with rare earth ions: Experiment and modeling, Opt. Mater. 34 (2012) 2055–2060. doi:10.1016/j.optmat.2012.04.007.

[31] D. Piątkowski, M. Schmidt, M. Twardowska, M. Nyk, J. Aizpurua, S. Maćkowski, Spectral Selectivity of Plasmonic Interactions between Individual Up-Converting Nanocrystals and Spherical Gold Nanoparticles, Materials. 10 (2017) 905. doi:10.3390/ma10080905.

[32] L. Novotny, B. Hecht, Principles of Nano-Optics, Cambridge University Press, 2006.

[33] Phys. Rev. B 62, 13174 (2000) - Interfacial shear force microscopy, (n.d.). https://journals.aps.org/prb/abstract/10.1103/PhysRevB.62.13174 (accessed March 23, 2018).

[34] A. Hartschuh, Tip-Enhanced Near-Field Optical Microscopy, Angew. Chem. Int. Ed. 47 (2008) 8178–8191. doi:10.1002/anie.200801605.

[35] N. Mauser, D. Piatkowski, T. Mancabelli, M. Nyk, S. Mackowski, A. Hartschuh, Tip Enhancement of Upconversion Photoluminescence from Rare Earth Ion Doped Nanocrystals, ACS Nano. 9 (2015) 3617–3626. doi:10.1021/nn504993e.

[36] D. Piatkowski, N. Hartmann, T. Macabelli, M. Nyk, S. Mackowski, A. Hartschuh, Silver nanowires as receiving-radiating nanoantennas in plasmon-enhanced up-conversion processes, Nanoscale. 7 (2015) 1479–1484. doi:10.1039/C4NR05209A.

[37] A.V. Zayats, I.I. Smolyaninov, A.A. Maradudin, Nano-optics of surface plasmon polaritons, Phys. Rep. 408 (2005) 131–314. doi:10.1016/j.physrep.2004.11.001.

[38] N. Hartmann, G. Piredda, J. Berthelot, G. Colas des Francs, A. Bouhelier, A. Hartschuh, Launching Propagating Surface Plasmon Polaritons by a Single Carbon Nanotube Dipolar Emitter, Nano Lett. 12 (2012) 177–181. doi:10.1021/nl203270b.

[39] M.A. Lieb, J.M. Zavislan, L. Novotny, Single-molecule orientations determined by direct emission pattern imaging, J. Opt. Soc. Am. B. 21 (2004) 1210–1215. doi:10.1364/JOSAB.21.001210.

[40] N. Hartmann, D. Piatkowski, R. Ciesielski, S. Mackowski, A. Hartschuh, Radiation Channels Close to a Plasmonic Nanowire Visualized by Back Focal Plane Imaging, ACS Nano. 7 (2013) 10257–10262. doi:10.1021/nn404611q.

[41] I. Gryczynski, J. Malicka, Z. Gryczynski, J.R. Lakowicz, Surface Plasmon-Coupled Emission with Gold Films, J. Phys. Chem. B. 108 (2004) 12568–12574. doi:10.1021/jp040221h.

[42] A. Prymaczek, M. Cwierzona, J. Grzelak, D. Kowalska, M. Nyk, S. Mackowski, D. Piatkowski, Remote activation and detection of up-converted luminescence via surface plasmon polaritons propagating in a silver nanowire, Nanoscale. 10 (2018) 12841–12847. doi:10.1039/C8NR04517H.

[43] D. Kowalska, B. Krajnik, M. Olejnik, M. Twardowska, N. Czechowski, E. Hofmann, S. Mackowski, Metal-Enhanced Fluorescence of Chlorophylls in Light-Harvesting Complexes Coupled to Silver Nanowires, Sci. World J. (2013). doi:10.1155/2013/670412.

[44] P. Bharadwaj, L. Novotny, Spectral dependence of single molecule fluorescence enhancement, Opt. Express. 15 (2007) 14266. doi:10.1364/OE.15.014266.

V. Other scientific/artistic achievements.

My scientific activity after PhD concerned first of all experimental research on various optically active hybrid nanostructures. The superior goal was to design and investigate nanostructures featuring new functionalities, which can be potentially interesting for practical applications. I was involved, for instance, in basic research on hybrid biological nanostructures. The main goal of this research was to increase efficiency of photosynthesis [u1][u2][u3]. I was also involved in experimental research on modern photovoltaic materials. In this project we modified spectroscopic properties of conducting polymers (components of a p-n junction) dedicated for photovoltaic applications. In the investigated hybrid system, the polymer has been activated by up-conversion nanocrystals. In this way, the polymer became sensitive to infrared radiation, which supplies significant part of the solar energy, that cannot be absorbed by silicon-based devices [u4]. My scientific activity concerned also development of modern nanomaterials, dedicated for biomedical [u5][u6] and optoelectronic applications [u7][u8]. For two years, I have also been involved in microscopic studies of hybrid nanostructures based on graphene. In the meantime, I have been developing semi-empirical computing methods useful for modeling both energy structure and absorption/emission spectra of rare earths doped materials [u9]. Results of my research alowed to describe luminescence processes occurring in various optoelectronical materials including scintillators [u10], anti-Stokes materials [u11], and telecommunication fiber amplifiers [u12].

Supplementary literature

[u1] Ł. Bujak, N. Czechowski, D. Piatkowski, R. Litvin, S. Mackowski, T.H.P. Brotosudarmo, R.J. Cogdell, S. Pichler, W. Heiss, Fluorescence enhancement of light-harvesting complex 2 from purple bacteria coupled to spherical gold nanoparticles, Appl. Phys. Lett. 99 (2011) 173701. doi:10.1063/1.3648113.

[u2] N. Czechowski, P. Nyga, M.K. Schmidt, T.H.P. Brotosudarmo, H. Scheer, D. Piatkowski, S. Mackowski, Absorption Enhancement in Peridinin–Chlorophyll–Protein Light-Harvesting Complexes Coupled to Semicontinuous Silver Film, Plasmonics. 7 (2012) 115–121. doi:10.1007/s11468-011-9283-7.

[u3] Ł. Bujak, M. Olejnik, T.H.P. Brotosudarmo, M.K. Schmidt, N. Czechowski, D. Piatkowski, J. Aizpurua, R.J. Cogdell, W. Heiss, S. Mackowski, Polarization control of metal-enhanced fluorescence in hybrid assemblies of photosynthetic complexes and gold nanorods, Phys. Chem. Chem. Phys. 16 (2014) 9015–9022. doi:10.1039/C3CP54364A.

[u4] J. Grzelak, K. Ciszak, M. Nyk, S. Mackowski, D. Piatkowski, Extending light-harvesting of poly(3-hexylthiophene) through efficient energy transfer from infra-red absorbing nanocrystals: Single nanoparticle study, Applied Physics Letters. 105 (2014) 163114. doi:10.1063/1.4900488.

[u5] I. Kamińska, K. Fronc, B. Sikora, M. Mouawad, A. Siemiarczuk, M. Szewczyk, K. Sobczak, T. Wojciechowski, W. Zaleszczyk, R. Minikayev, W. Paszkowicz, P. Stępień, P. Dziawa, K. Ciszak, D. Piątkowski, S. Maćkowski, M. Kaliszewski, M. Włodarski, J. Młyńczak, K. Kopczyński, M. Łapiński, D. Elbaum, Upconverting/magnetic: Gd2O3:(Er3+,Yb3+,Zn2+) nanoparticles for biological applications: effect of Zn2+ doping, RSC Adv. 5 (2015) 78361–78373. doi:10.1039/C5RA11888C.

[u6] D. Wawrzynczyk, D. Piatkowski, S. Mackowski, M. Samoc, M. Nyk, Microwave-assisted synthesis and single particle spectroscopy of infrared down- and visible up-conversion in Er3+ and Yb3+ co-doped fluoride nanowires, J. Mater. Chem. C. 3 (2015) 5332–5338. doi:10.1039/C5TC00468C.

[u7]   H. Labiadh, T.B. Chaabane, D. Piatkowski, S. Mackowski, J. Lalevée, J. Ghanbaja, F. Aldeek, R. Schneider, Aqueous route to color-tunable Mn-doped ZnS quantum dots, Materials Chemistry and Physics. 140 (2013) 674–682. doi:10.1016/j.matchemphys.2013.04.023.

[u8]   A. Schejn, L. Balan, D. Piatkowski, S. Mackowski, J. Lulek, R. Schneider, From visible to white-light emission by siloxane-capped ZnO quantum dots upon interaction with thiols, Optical Materials. 34 (2012) 1357–1361. doi:10.1016/j.optmat.2012.02.030.

[u9]   D. Piatkowski, S. Mackowski, Excited state absorption in glasses activated with rare earth ions: Experiment and modeling, Optical Materials. 34 (2012) 2055–2060. doi:10.1016/j.optmat.2012.04.007.

[u10]   A.J. Wojtowicz, S. Janus, D. Piatkowski, Fast and efficient VUV/UV emissions from (Ba,La)F2:Er crystals, Journal of Luminescence. 129 (2009) 1594–1597. doi:10.1016/j.jlumin.2009.01.020.

[u11]   P. Stremplewski, C. Koepke, D. Piątkowski, Verification of upconversion in ZBLAN:Ho3+ glass under photon-avalanche-type excitation at 980 nm, Appl. Phys. B. 107 (2012) 171–176. doi:10.1007/s00340-011-4846-z.

[u12]   P. Stremplewski, C. Koepke, D. Piatkowski, M. Rozanski, Nonmonotonic saturation characteristic and excited state absorption in long optical fiber, Appl. Phys. B. 103 (2011) 123–128. doi:10.1007/s00340-010-4198-0.